Anisotropic interaction potential between a Rydberg electron and an open-shell ion

William Clark, Chris H. Greene, and Gregory Miecznik
JILA and the Department of Physics, University of Colorado, Boulder, Colorado 80309-0440
(Received 10 October 1995)

We develop a theoretical description of the anisotropic interaction between a Rydberg electron and an ionic core. An adiabatic formulation expresses the anisotropic nature of the interaction through angular-momentum operators of the core and the Rydberg electron. Terms with odd tensorial structure, such as a vector hyperpolarization proportional to $\vec{L}_c \cdot \vec{\ell}$, emerge in the long-range potential. Computed energies of neon $n=10$ Rydberg states are compared with recent experimental measurements. The vector term improves agreement between theory and experiment. The vector hyperpolarizability is calculated explicitly, along with some standard polarizabilities of Ne^+.

PACS number(s): 34.20.Cf, 34.60.+z

I. INTRODUCTION

While numerous analyses have treated a charged particle in the field of a closed-shell atom or ion [1–3], theory has contributed far less to the interpretation of the anisotropic interactions between a charge and an open-shell species. Zygelman [4] published one of the most recent derivations of the interaction potential between a charge and an open-shell core with unit angular momentum ($L_c=1$). The Ref. [4] analysis used somewhat unfamiliar methods to predict a different, counterintuitive ''spin-orbit-type potential,'' proportional to

$$\frac{\vec{L}_c \cdot \vec{\ell}}{r^6}, \tag{1}$$

where r is the distance between the charge and the core and $\vec{\ell}$ is the orbital angular-momentum operator of the charged particle with respect to the center of mass. This unusual potential, purely electrostatic in nature despite the spin-orbit-type structure, was not given fully in Ref. [4] and its physical origin has remained somewhat unclear. For instance, a geometric (Berry-type) phase arose in the Ref. [4] derivation, in addition to non-Abelian gauge fields that are representation dependent.

In Sec. II of this paper we reformulate the conventional adiabatic derivation [5] of the large-r potential between a Rydberg electron and an open-shell ionic core. The adiabatic formulation is then improved in Sec. III by developing an effective radial Hamiltonian that can be treated diabatically within a small physically relevant channel subspace. The two derivations, which borrow techniques from a paper by Fano and Macek [6], express the anisotropy of the long-range interactions in terms of tensorial operators that are appropriate to the adiabatic and diabatic formulations. Specifically, the anisotropy of the long-range adiabatic potential is expressed in terms of angular-momentum operators of the core and of the Rydberg electron, while the anisotropy of the effective Hamiltonian is expressed in terms of a defined set of ''unit tensorial operators'' that also operate separately on the core and the Rydberg electron, but correctly account for the coupling between the diabatic channels. The final forms we obtain confirm the existence of vector terms proportional to r^{-6}. A r^{-6} term proportional to $\vec{L}_c \cdot \vec{\ell}$ is shown to arise in cases where L_c is a good quantum number, such as in low-Z atomic Rydberg systems. Moreover, additional operators with tensorial rank $k \geqslant 1$ contribute in an important way to the r^{-3}, r^{-4}, r^{-5}, and r^{-6} potentials. All terms are given explicitly and can be subjected to direct experimental tests. Our final forms for the large-r potential and effective Hamiltonian show that such terms arise naturally in conventional derivations of the electron-ion interaction. Specifically, their appearance is not contingent upon the introduction of a geometric (Berry's) phase, nor on a non-Abelian gauge field of the type used in Ref. [4].

Furthermore, in Sec. III we compare calculated energy levels, found by diagonalizing our parametrized effective Hamiltonian in a Sturmian basis, with experimentally observed levels for $n=10$ Rydberg states of neon [7]. Inclusion of the vector term results in a significant shift of the low-ℓ Rydberg state energies, improving agreement between calculated and observed energy levels. An alternative method for extracting polarizabilities from measured Rydberg energy-level spectra based on this diagonalization is discussed and applied. Finally, a calculation of the vector hyperpolarizability term is presented along with the standard dipole scalar and (second-rank) tensor polarizabilities.

II. ADIABATIC FORMULATION

As in Ref. [5], we use an adiabatic representation of the asymptotic close-coupling (CC) equations for an electron in the field of an ionic core. Only the radial *distance* is treated adiabatically in this derivation, in contrast to Ref. [4], which further adiabatizes the angular coordinates of the charge, as in standard molecular Born-Oppenheimer formulations. In view of the fact that experimental Rydberg level spectra are frequently probed for nonpenetrating, high-ℓ states, we adopt the usual $(J_c \ell)K$ coupling scheme [8] and ignore the spin of the outermost (Rydberg) electron. (The spin of the outermost electron is most important in the context of exchange, which we neglect here.) Atomic units are used throughout this paper.

The interaction of a Rydberg electron with an ionic core is represented by a long-range coupling matrix characteristic of

 © 1996 The American Physical Society

the standard close-coupling equations without exchange. An expansion of the total wave function Ψ in an r-independent basis $\{\phi_i(\omega)\}$, formed from coupled core states and orbital functions of the Rydberg electron, gives the coupling matrix

$$V_{ij}^{\mathrm{CC}}(r)=\left(\frac{\ell_i(\ell_i+1)}{2r^2}-\frac{1}{r}+E_i\right)\delta_{ij}+V_{ij}(r), \tag{2}$$

where $V_{ij}(r)$ are the electrostatic matrix elements $\langle\phi_i|V|\phi_j\rangle$, E_i is the ionic energy level in channel i, and ℓ_i is the orbital angular momentum of the Rydberg electron. In this paper matrix elements involve integrals over all coordinates (ω) (and traces over all spins) in the problem, except for the radial coordinate of the Rydberg electron.

The adiabatic potentials $U_\mu(r)$ and eigenvectors $\Phi_\mu(r)$ are obtained by solving the linear eigensystem at each r

$$\underline{H}^{\mathrm{CC}}(r)\underline{\Phi}_\mu(r)=U_\mu(r)\underline{\Phi}_\mu(r), \tag{3}$$

where $\underline{H}^{\mathrm{CC}}(r)=\underline{V}^{\mathrm{CC}}(r)$. Within this adiabatic representation $\{\underline{\Phi}_\mu(r)\}$ the radial close-coupling equations take the form

$$\left[-\frac{1}{2}\left(\underline{I}\frac{d}{dr}+\underline{P}(r)\right)^2-[E\underline{I}-\underline{U}(r)]\right]F(r)=\underline{0}, \tag{4}$$

where I is the identity matrix, F is the radial solution matrix, and the nonadiabatic (derivative) coupling matrix is

$$P_{\mu\nu}(r)=\left\langle\Phi_\mu\left|\frac{\partial}{\partial r}\Phi_\nu\right.\right\rangle=\left(\underline{\Phi}^T(r)\frac{d}{dr}\underline{\Phi}(r)\right)_{\mu\nu}. \tag{5}$$

Here the adiabatic channels are labeled by greek letters; they converge as $r\to\infty$ to the ionic channels labeled by latin letters.

For Rydberg systems with large n and ℓ quantum numbers, the small values of $V_{ij}(r)$ compared to E_i-E_j allow us to perform the diagonalization of $\underline{H}^{\mathrm{CC}}(r)$ perturbatively. An important step in this perturbative diagonalization is the inclusion of the diagonal matrix elements $V_{ii}(r)$ in the unperturbed Hamiltonian [5]. This is completely general and transparent when the long-range coupling matrix is written as

$$V_{ij}^{\mathrm{CC}}(r)=\left(\frac{\ell_i(\ell_i+1)}{2r^2}-\frac{1}{r}+E_i+V_{ii}(r)\right)\delta_{ij}+V_{ij}(r), \tag{6}$$

where $V_{ij}(r)$ are now purely off-diagonal contributions. Provided there are no degenerate states of the ion with opposite parity [9,10], this perturbative series gives a long-range adiabatic potential $U_\mu(r)$. In addition, we include nonadiabatic effects perturbatively using the post-adiabatic theory of Klar and Fano [11–13], which modifies $U_\mu(r)$ by

$$\bar{U}_\mu(r)\simeq U_\mu(r)-\frac{1}{2}(P^2)_{\mu\mu}+2(E-U_\mu)\sum_\nu\frac{|P_{\mu\nu}|^2}{U_\mu-U_\nu}. \tag{7}$$

where the perturbative condition $P_{\mu\nu}^2\ll|U_\mu-U_\nu|$ is always satisfied for Rydberg systems with sufficiently large n and ℓ. The perturbative diagonalization of H^{CC}, up to second order in $V_{\mu\nu}$, produces terms involving summations over intermediate channels ν with potential energy difference denominators $U_\mu-U_\nu$. These contributions can be classified as either degenerate or nondegenerate depending on whether an intermediate channel ν is degenerate with the physically relevant channel ν at $r\to\infty$ (i.e., $U_\nu=U_\mu$).

A. Nondegenerate contributions

In the nondegenerate case, for which no intermediate channel ν is degenerate with the physically relevant channel μ at $r\to\infty$ (i.e., $E_\nu\neq E_\mu$), this approach gives a long-range potential (nondegenerate contributions) with the structure

$$\bar{U}_\mu(r)=E_\mu-\frac{1}{r}+\frac{\ell_\mu(\ell_\mu+1)}{2r^2}+\frac{Q_{\mu\mu}^{(2)}}{r^3}-\frac{\alpha_\mu}{2r^4}+\frac{Q_{\mu\mu}^{(4)}}{r^5}+\frac{\beta_\mu^{\mathrm{ad}}+\beta_\mu^{\mathrm{nad}}-2(E-E_\mu)\lambda_\mu-\delta_\mu-\eta_\mu}{2r^6}+O(r^{-8}), \tag{8}$$

where ad (nad) denotes adiabatic (nonadiabatic). Every term in this potential can be written as a standard second-order perturbation sum, except for the diagonal quadrupole $Q_{\mu\mu}^{(2)}$ and hexadecapole $Q_{\mu\mu}^{(4)}$ terms, which are diagonal (first-order) matrix elements of the ionic electric quadrupole and hexadecapole operators. Explicit expressions for these terms as infinite perturbation sums, over bound and continuum states of the core, can be obtained along the lines of the derivation given by Ref. [5], although there are differences in notation, in coupling scheme, and in the multipoles that were included. Each term $Q_{\mu\mu}^{(2)}$, $Q_{\mu\mu}^{(4)}$, α_μ, β_μ^{ad}, β_μ^{nad}, λ_μ, δ_μ, and η_μ depends on the various quantum numbers J_c, ℓ, and K in a relatively complicated fashion that is difficult to analyze

$$Q_{\mu\nu}^{(k)}=\left\langle\mu\left|\sum_{i=1}^{N_c}r_i^kP_k(\cos\theta_{Ri})\right|\nu\right\rangle, \tag{9}$$

$$\alpha_\mu=\sum_{\nu\neq\mu}\frac{2Q_{\mu\nu}^{(1)}Q_{\nu\mu}^{(1)}}{E_\nu-E_\mu}, \tag{10}$$

$$\beta_\mu^{\mathrm{ad}}=\sum_{\nu\neq\mu}\frac{[\ell_\nu(\ell_\nu+1)-\ell_\mu(\ell_\mu+1)]}{(E_\nu-E_\mu)^2}Q_{\mu\nu}^{(1)}Q_{\nu\mu}^{(1)}, \tag{11}$$

$$\beta_\mu^{\mathrm{nad}}=\sum_{\nu\neq\mu}\frac{4Q_{\mu\nu}^{(1)}Q_{\nu\mu}^{(1)}}{(E_\nu-E_\mu)^2}, \tag{12}$$

$$\lambda_\mu=\sum_{\nu\neq\mu}\frac{8Q_{\mu\nu}^{(1)}Q_{\nu\mu}^{(1)}}{(E_\nu-E_\mu)^3}, \tag{13}$$

$$\delta_\mu=\sum_{\nu\neq\mu}\frac{2Q_{\mu\nu}^{(2)}Q_{\nu\mu}^{(2)}}{E_\nu-E_\mu}, \tag{14}$$

and

$$\eta_\mu=\sum_{\nu\neq\mu}\frac{4Q_{\mu\nu}^{(1)}Q_{\nu\mu}^{(3)}}{E_\nu-E_\mu}. \tag{15}$$

In Eq. (9) N_c denotes the number of ionic core electrons, while the subscript R refers the Rydberg electron. One consequence of including nonadiabatic effects is the appearance of an energy-dependent term in the long-range potential. This energy dependence has generated a small controversy because different treatments disagree in multiplicative constants [1,3]. Reference [3] shows, however, that the energy-dependent term of order r^{-6} can be written as an ℓ-dependent linear combination of r^{-7} and r^{-8}, implying that the energy-dependent term can be regarded as a contribution of higher order than r^{-6}.

To reveal the operator structure and to clarify the dependence of each term on J_c, ℓ, and K, we disentangle each term using recoupling algebra and place each in the form

$$\sum_k (-1)^k \langle X^{(k)} \cdot Y^{(k)} \rangle_\mu , \tag{16}$$

where $X^{(k)}$ operates on the ionic core while $Y^{(k)}$ operates on the Rydberg electron. The validity of this derivation relies on the fact that the infinite sum over intermediate states ν in Eqs. (10)–(15) is itself a ''scalar'' object that contributes no multipolarity to any term. For example, the dipole polarizability α_μ and the $\beta_\mu^{\rm ad}$ term are proportional to the expectation value, in $|\mu\rangle$, of

$$(r_c^{(1)} \cdot r_R^{(1)}) P (r'^{(1)}_c \cdot r'^{(1)}_R), \tag{17}$$

where P is a weighted (scalar) projection operator. Using standard Wigner-Racah algebra this is recoupled into the structure

$$\sum_k (-1)^k [r_c^{(1)} \otimes P_c r'^{(1)}_c]^{(k)} \cdot [r_R^{(1)} \otimes P_R r'^{(1)}_R]^{(k)}, \tag{18}$$

in which terms appear with net multipole moment k acting on the core and Rydberg electron, respectively. Here the projection operator P has been factored into scalar operators P_c and P_R that project onto the ionic core states and the states of the Rydberg electron, respectively.

Following the spirit of the Fano-Macek [6] treatment of alignment and orientation, we replace the above tensorial structure by coupled angular-momentum operators of the same rank. Each such replacement introduces a compensating ratio of reduced matrix elements

$$\sum_k (-1)^k \frac{\langle \mu \| X^{(k)} \cdot Y^{(k)} \| \mu \rangle}{\langle \mu \| J_c^{(k)} \cdot \ell^{(k)} \| \mu \rangle} \langle J_c^{(k)} \cdot \ell^{(k)} \rangle_\mu$$

$$= \sum_k C_k \langle J_c^{(k)} \cdot \ell^{(k)} \rangle_\mu . \tag{19}$$

Here the choice of the $J_c^{(k)} \cdot \ell^{(k)}$ operator representation is motivated by the fact that adiabatic potentials involve specific values of J_c and ℓ_μ. In general, the choice of a particular operator representation depends on whether the formulation is adiabatic or diabatic. In the diabatic formulation of Sec. III a ''unit tensorial operator'' notation is defined that correctly accounts for the coupling between the diabatic channels; this coupling cannot be represented by the angular-momentum operator representation used in this section.

Keeping powers of r^{-1} up to r^{-6} and grouping terms of the same tensorial structure allows us to present the long-range potential (nondegenerate contributions) in a form that emphasizes its anisotropic nature

$$\begin{aligned} \bar{U}_\mu(r) = E_\mu - \frac{1}{r} + \frac{\ell_\mu(\ell_\mu+1)}{2r^2} + \frac{C^{4\mu}_{0(1,1)}}{r^4} \\ + \frac{C^{6\mu}_{0[(1,1),(2,2)]}}{r^6} + \frac{C^{6\mu}_{1(1,1)}}{r^6} \langle J_c^{(1)} \cdot \ell^{(1)} \rangle_\mu \\ + \left[\frac{C^{3\mu}_{2(2,0)}}{r^3} + \frac{C^{4\mu}_{2(1,1)}}{r^4} + \frac{C^{6\mu}_{2[(1,1),(2,2),(1,3)]}}{r^6} \right] \langle J_c^{(2)} \cdot \ell^{(2)} \rangle_\mu \\ + \left[\frac{C^{5\mu}_{4(4,0)}}{r^5} + \frac{C^{6\mu}_{4[(2,2),(1,3)]}}{r^6} \right] \langle J_c^{(4)} \cdot \ell^{(4)} \rangle_\mu . \end{aligned} \tag{20}$$

Here the terms $C^{n\mu}_{k(a,b)}$, corresponding to *even* tensorial rank k, order n in r^{-1}, and with a-multipole and b-multipole contributions, are given by

$$\begin{aligned} C^{n\mu}_{k(a,b)} = \frac{(-1)^{2J_c+\ell_\mu}(2\ell_\mu+1)(2k+1)}{\langle \ell_\mu \| \ell^{(k)} \| \ell_\mu \rangle \langle J_c \| J_c^{(k)} \| J_c \rangle} \{\ell_\mu, \ell_\mu, k\} \\ \times \{a,b,k\} \sum_{\gamma_\nu, J_\nu} \Gamma^n_k(a,b) \begin{Bmatrix} a & b & k \\ J_c & J_c & J_\nu \end{Bmatrix} \\ \times \left\langle \gamma_c J_c \left\| \sum_{i=1}^{N_c} r_i^a C^{(a)}(\hat{r}_i) \right\| \gamma_\nu J_\nu \right\rangle \\ \times \left\langle \gamma_\nu J_\nu \left\| \sum_{j=1}^{N_c} r_j^b C^{(b)}(\hat{r}_j) \right\| \gamma_c J_c \right\rangle , \end{aligned} \tag{21}$$

where $C^{(a)}(\hat{r}_i)$ are renormalized spherical harmonics and

$$\{x,y,z\} = \begin{pmatrix} x & y & z \\ 0 & 0 & 0 \end{pmatrix} \tag{22}$$

is our condensed notation for 3-j symbols whose magnetic quantum numbers vanish. Terms that share the same tensorial rank and power of r^{-1} but differ in multipole dependence are combined into

$$C^{n\mu}_{k[(a_1,b_1),(a_2,b_2),\ldots]} = C^{n\mu}_{k(a_1,b_1)} + C^{n\mu}_{k(a_2,b_2)} + \cdots . \tag{23}$$

The matrix elements $\langle J_c^{(k)} \cdot \ell^{(k)} \rangle_\mu$ are

$$\begin{aligned} \langle J_c^{(k)} \cdot \ell^{(k)} \rangle_\mu &= \langle (J_c \ell_\mu) K | J_c^{(k)} \cdot \ell^{(k)} | (J_c \ell_\mu) K \rangle \\ &= (-1)^{J_c+\ell_\mu+K} \begin{Bmatrix} J_c & \ell_\mu & K \\ \ell_\mu & J_c & k \end{Bmatrix} \langle J_c \| J_c^{(k)} \| J_c \rangle \\ &\quad \times \langle \ell_\mu \| \ell^{(k)} \| \ell_\mu \rangle , \end{aligned} \tag{24}$$

[14,15] and explicit expressions for particular $\Gamma^n_k(a,b)$'s with even k in Eq. (19) are given by

$$\Gamma^3_k(2,0) = \Gamma^5_k(4,0) = 1, \tag{25}$$

$$\Gamma_k^4(1,1)=\Gamma_k^6(2,2)=\frac{1}{E_\mu-E_\nu}, \tag{26}$$

$$\Gamma_k^6(1,3)=2\Gamma_k^4(1,1), \tag{27}$$

$$\Gamma_0^6(1,1)=\frac{6}{2(E_\nu-E_\mu)^2}-\frac{8(E-E_\mu)}{(E_\nu-E_\mu)^3}, \tag{28}$$

and

$$\Gamma_2^6(1,1)=\frac{3}{2(E_\nu-E_\mu)^2}-\frac{8(E-E_\mu)}{(E_\nu-E_\mu)^3}. \tag{29}$$

The term $C^{6\mu}_{1(1,1)}$ is the only one with *odd* tensorial rank k $(k=1)$

$$C^{6\mu}_{1(1,1)}=(-1)^{2J_c}\frac{\sqrt{6}}{\langle J_c\|J_c^{(1)}\|J_c\rangle}\sum_{\gamma_\nu,J_\nu}\frac{1}{2(E_\nu-E_\mu)^2}\begin{Bmatrix}1&1&1\\J_c&J_c&J_\nu\end{Bmatrix}\left\langle\gamma_cJ_c\left\|\sum_{i=1}^{N_c}r_iC^{(1)}(\hat r_i)\right\|\gamma_\nu J_\nu\right\rangle\left\langle\gamma_\nu J_\nu\left\|\sum_{j=1}^{N_c}r_jC^{(1)}(\hat r_j)\right\|\gamma_cJ_c\right\rangle. \tag{30}$$

In contrast to the long-range potential presented in Eq. (8), the operator form of the anisotropic potential in Eq. (20) possesses a very simple dependence on the various quantum numbers J_c, ℓ, and K. Along with the factorization of the orbital angular momentum ℓ of the Rydberg electron from information pertaining to the ionic core, all terms of the same *even* tensorial rank k share the same ℓ dependence. In addition, all dependence on K appears in a single 6-j symbol originating from the matrix element $\langle J_c^{(k)}\cdot\ell^{(k)}\rangle_\mu$ and accounts for the splitting of the $|K+J_c|-|K-J_c|+1$ number of ℓ levels of common K. Unfortunately, the terms $C^{n\mu}_{k(a_1,b_1)}, C^{n\mu}_{k(a_2,b_2)},\ldots$ that make up $C^{n\mu}_{k[(a_1,b_1),(a_2,b_2),\ldots]}$ are not distinguishable from one another since they share the same tensorial rank, power of r^{-1}, and ℓ dependence.

The angular-momentum representation of the long-range potential in Eq. (20) immediately shows the appearance of a vector contribution whose structure is similar to a term predicted by Zygelman [4]. Moreover, we are able to give an explicit expression for each term and to explain its physical origin. For instance, the vector contribution depends on the dipole moments of the ionic core and its existence hinges on the centrifugal repulsion experienced by the Rydberg electron. It is the presence of the $\ell_\nu(\ell_\nu+1)$ term in $\beta_\mu^{\rm ad}$ that makes the $C^{6\mu}_{1(1,1)}$ term nonzero. Terms in the untransformed potential in Eq. (8) without such an additional ℓ_ν dependence are incapable of giving rise to odd tensorial contributions such as $J_c^{(1)}\cdot\ell^{(1)}$. Specifically, if there is no additional ℓ_ν dependence the summation over ℓ_ν is easily performed:

$$\begin{aligned}\sum_{\ell_\nu}&(-1)^{\ell_\nu}(2\ell_\nu+1)\{\ell_\mu,a,\ell_\nu\}\\&\times\{\ell_\nu,b,\ell_\mu\}\begin{Bmatrix}a&b&k\\\ell_\mu&\ell_\mu&\ell_\nu\end{Bmatrix}\\&=(-1)^{a+b-k}\begin{pmatrix}a&b&k\\0&0&0\end{pmatrix}\begin{pmatrix}\ell_\mu&\ell_\mu&k\\0&0&0\end{pmatrix}.\end{aligned} \tag{31}$$

Since each contribution to our long-range potentials involves a and b values that add up to an even number, the tensorial rank k must be even in this case. Thus, unless a particular term in Eq. (8) has some additional ℓ_ν dependence, such as $\ell_\nu(\ell_\nu+1)$, the above summation shows that only even tensorial terms will appear in the anisotropic potentials.

We can understand the vector potential in another way by recognizing that $\beta_\mu^{\rm ad}$ can be written as

$$\begin{aligned}\beta_\mu^{\rm ad}&=\sum_{\nu\neq\mu}\frac{[\ell_\nu(\ell_\nu+1)-\ell_\mu(\ell_\mu+1)]}{(E_\nu-E_\mu)^2}Q^{(1)}_{\mu\nu}Q^{(1)}_{\nu\mu}\\&=\sum_{\nu\neq\mu}\frac{\langle\mu|[\hat r_R,\vec\ell^{\,2}]\cdot\vec r_c|\nu\rangle\langle\nu|\hat r_R'\cdot\vec r_c'|\mu\rangle}{(E_\nu-E_\mu)^2}.\end{aligned} \tag{32}$$

The commutator of $\hat r_R$ and $\vec\ell^{\,2}$ is

$$[\hat r_R,\vec\ell^{\,2}]=i(\vec\ell\times\hat r_R-\hat r_R\times\vec\ell) \tag{33}$$

and with a little recoupling the vector contribution of $\beta_\mu^{\rm ad}$ becomes proportional to

$$([\hat r_R,\vec\ell^{\,2}]\times P_R\hat r_R')\cdot(\vec r_c\times P_c\vec r_c'). \tag{34}$$

Using

$$\begin{aligned}[\hat r_R,\vec\ell^{\,2}]\times P_R\hat r_R'=&-2i(\hat r_R\cdot P_R\hat r_R')\vec\ell+2i\hat r_R(\vec\ell\cdot P_R\hat r_R')\\&-2\hat r_R\times P_R\hat r_R',\end{aligned} \tag{35}$$

we see that an r^{-6} vector interaction proportional to

$$\sim\vec\ell\cdot(\vec r_c\times P_c\vec r_c') \tag{36}$$

immediately appears. The existence of this vector interaction hinges on the presence of the centrifugal term within $\beta_\mu^{\rm ad}$. In addition, the right-hand side of Eq. (33) indicates that the Rydberg electron exerts a torque on the ionic core.

B. Degenerate contributions

The nature of the long-range effective potential changes qualitatively when degenerate terms are considered. Degenerate contributions appear when intermediate channels ν share the same threshold $E_\nu=E_\mu$, K value, and parity with the physically relevant channels μ at $r\to\infty$. For simplicity we assume, however, that the intermediate orbital angular mo-

menta l_ν differ from l_μ. A derivation similar to that given above produces a long-range adiabatic potential with the structure

$$U_\mu(r)=E_\mu-\frac{1}{r}+\frac{\ell_\mu(\ell_\mu+1)}{2r^2}+\frac{Q^{(2)}_{\mu\mu}}{r^3}+\frac{a_\mu}{r^4}+\frac{Q^{(4)}_{\mu\mu}}{r^5}+\frac{b_\mu}{r^6}+O(r^{-8}), \tag{37}$$

where the a_μ and b_μ terms are explicitly

$$a_\mu=\sum_{\nu\neq\mu}\frac{2Q^{(2)}_{\mu\nu}Q^{(2)}_{\nu\mu}}{\ell_\mu(\ell_\mu+1)-\ell_\nu(\ell_\nu+1)} \tag{38}$$

and

$$b_\mu=\sum_{\nu\neq\mu}\frac{4Q^{(2)}_{\mu\nu}Q^{(4)}_{\nu\mu}}{\ell_\mu(\ell_\mu+1)-\ell_\nu(\ell_\nu+1)}. \tag{39}$$

Again we recouple to reveal the tensorial structure and then replace the tensorial structure with coupled angular-momentum operators of the same rank. Keeping powers of r^{-1} up to r^{-6} and grouping terms of the same tensorial rank allows us to present the long-range potential (degenerate contributions) in a form that emphasizes its anisotropic nature:

$$\begin{aligned}U_\mu(r)=E_\mu&-\frac{1}{r}+\frac{\ell_\mu(\ell_\mu+1)}{2r^2}+\frac{D^{4\mu}_{0(2,2)}}{r^4}+\frac{D^{4\mu}_{1(2,2)}}{r^4}\langle J_c^{(1)}\cdot\ell^{(1)}\rangle_\mu\\&+\left[\frac{D^{3\mu}_{2(2,0)}}{r^3}+\frac{D^{4\mu}_{2(2,2)}}{r^4}+\frac{D^{6\mu}_{2(2,4)}}{r^6}\right]\langle J_c^{(2)}\cdot\ell^{(2)}\rangle_\mu\\&+\left[\frac{D^{4\mu}_{3(2,2)}}{r^4}+\frac{D^{6\mu}_{3(2,4)}}{r^6}\right]\langle J_c^{(3)}\cdot\ell^{(3)}\rangle_\mu\\&+\left[\frac{D^{4\mu}_{4(2,2)}}{r^4}+\frac{D^{5\mu}_{4(4,0)}}{r^5}+\frac{D^{6\mu}_{4(2,4)}}{r^6}\right]\langle J_c^{(4)}\cdot\ell^{(4)}\rangle_\mu\\&+\frac{D^{6\mu}_{5(2,4)}}{r^6}\langle J_c^{(5)}\cdot\ell^{(5)}\rangle_\mu+\frac{D^{6\mu}_{6(2,4)}}{r^6}\langle J_c^{(6)}\cdot\ell^{(6)}\rangle_\mu.\end{aligned} \tag{40}$$

Here the terms $D^{n\mu}_{k(a,b)}$ corresponding to tensorial rank k, order n in r^{-1}, and with a-multipole and b-multipole contributions are given by

$$\begin{aligned}D^{n\mu}_{k(a,b)}=&\frac{(-1)^{k+2J_c+\ell_\mu}(2k+1)(2\ell_\mu+1)}{\langle\ell_\mu\|\ell^{(k)}\|\ell_\mu\rangle\langle J_c\|J_c^{(k)}\|J_c\rangle}\sum_{\ell_\nu}\Delta^n_{\mu\nu}(a,b)\\&\times(-1)^{\ell_\nu}(2\ell_\nu+1)\{\ell_\mu,a,\ell_\nu\}\{\ell_\nu,b,\ell_\mu\}\\&\times\begin{Bmatrix}a&b&k\\\ell_\mu&\ell_\mu&\ell_\nu\end{Bmatrix}\begin{Bmatrix}a&b&k\\J_c&J_c&J_c\end{Bmatrix}\\&\times\left\langle\gamma_cJ_c\left\|\sum_{i=1}^{N_c}r_i^aC^{(a)}(\hat r_i)\right\|\gamma_cJ_c\right\rangle\\&\times\left\langle\gamma_cJ_c\left\|\sum_{j=1}^{N_c}r_j^bC^{(b)}(\hat r_j)\right\|\gamma_cJ_c\right\rangle,\end{aligned} \tag{41}$$

where the $\Delta^n_{\mu\nu}(a,b)$'s are

$$\Delta^3_{\mu\nu}(2,0)=\Delta^5_{\mu\nu}(4,0)=1, \tag{42}$$

$$\Delta^4_{\mu\nu}(2,2)=\frac{2}{\ell_\mu(\ell_\mu+1)-\ell_\nu(\ell_\nu+1)}, \tag{43}$$

$$\Delta^6_{\mu\nu}(2,4)=2\Delta^4_{\mu\nu}(2,2). \tag{44}$$

Like the nondegenerate terms these $D^{n\mu}_{k(a,b)}$ exhibit a factorization of contributions pertaining to the ionic core and the Rydberg electron. In contrast to the nondegenerate case, though, terms with the same tensorial rank k now differ in their ℓ dependence. This explicit dependence of the various terms on the Rydberg electron angular momentum cannot be neglected when measurements are performed on various systems.

Each term in this potential depends on quadrupole and/or hexadecapole moments of the ionic core along with reciprocal powers of $\ell_\mu(\ell_\mu+1)-\ell_\nu(\ell_\nu+1)$. As a consequence, these terms will tend to be fairly small in comparison to those in the nondegenerate case, but may still play an important role in accurately describing Rydberg spectra. The contribution to the vector term depends on quadrupole moments of the ionic core and, similar to the nondegenerate case, arises because of the centrifugal repulsion experienced the Rydberg electron. In addition, we see that odd tensorial terms with ranks of 3 and 5 arise in this case along with expected even tensorial terms with ranks of 4 and 6. Even though the degenerate contributions have been derived separately from the nondegenerate ones, a full account of the interaction between a Rydberg electron and an anisotropic ionic core must involve all terms in Eq. (20) plus any terms not duplicated in Eq. (37).

III. BEYOND THE ADIABATIC APPROXIMATION

The potentials presented above are simply long-range adiabatic potentials with some post-adiabatic corrections. In this section we go beyond a pure adiabatic formulation and derive an effective radial Hamiltonian with an interaction potential that has a parametrized form, includes coupling, and is valid for the typically large values of r in high-n and -ℓ Rydberg systems. With such a Hamiltonian both energy levels and dynamical information about Rydberg systems can be found by solving a set of coupled radial equations where the interaction of the Rydberg electron with the core is accounted for by the parameters in the interaction potential. It is preferable to stay away from a purely adiabatic formulation since derivative couplings are numerically difficult to handle near close avoided crossings, expected to occur ubiquitously in open-shell atoms with fine structure. However, it is expected that such an effective Hamiltonian should yield the same long-range adiabatic potentials presented in Sec. II in the limit of large r.

Here we partition the various diabatic channels into a P set that is coupled together to form a total angular momentum K (excluding the Rydberg electron spin) and parity π and its complementary Q set. The P set includes all channels that converge to thresholds that are physically relevant to the

description of a particular Rydberg system. With this partition the close-coupling equations take the form

$$\left[-\frac{1}{2}\underline{I}\frac{d^2}{dr^2}-E\underline{I}+\begin{pmatrix} V^{QQ} & V^{QP} \\ V^{PQ} & V^{PP}\end{pmatrix}\right]\begin{pmatrix} F^Q \\ F^P\end{pmatrix}=0, \tag{45}$$

where V is the coupling matrix V^{CC} in Eq. (2). Eliminating F^Q [16], the effective Hamiltonian acting on F^P can be written formally as

$$H^{PP}_{\mathrm{eff}}=-\frac{1}{2}I^{PP}\frac{d^2}{dr^2}+V^{PP}-V^{PQ}\frac{1}{h^{QQ}}V^{QP}, \tag{46}$$

where

$$h^{QQ}=-\frac{1}{2}I^{QQ}\frac{d^2}{dr^2}-EI^{QQ}+V^{QQ}. \tag{47}$$

Since we are interested in high-n and -ℓ Rydberg systems, the energy E will always be near one of thresholds that are split by fine structure in the P subspace. Thus E can be written as

$$E=E_{P_0}+c_{P_0}(E), \tag{48}$$

where, for convenience, E_{P_0} is chosen to be the energy of the lowest threshold in the P subspace and $c_{P_0}(E)$ is a small energy-dependent parameter. In addition, it is reasonable to expect that the radial kinetic energy of a Rydberg electron in a high-n and -ℓ state will be a small quantity. Thus the inverse of h^{QQ} can be expanded in $c_{P_0}(E)$ and $-1/2\,I^{QQ}d^2/dr^2$. Moreover, to ensure that the effective Hamiltonian $H^{PP}_{\mathrm{eff}}(r)$ yields the same long-range adiabatic potentials as in Sec. II, we add and subtract the small quantity $-1/r+\ell_{P_0}(\ell_{P_0}+1)/2r^2$ from E. Then,

$$E=E_{P_0}-\frac{1}{r}+\frac{\ell_{P_0}(\ell_{P_0}+1)}{2r^2}+\epsilon_{P_0}(E,r), \tag{49}$$

where the parameter $\epsilon_{P_0}(E,r)$ is simply c_{P_0} minus the term added and subtracted from E and ℓ_{P_0} is the orbital angular momentum of the Rydberg electron in the lowest channel converging to E_{P_0}.

Expanding in $-1/2\,I^{QQ}d^2/dr^2-\epsilon_{P_0}(E,r)I^{QQ}$ and neglecting terms higher than second order in the coupling matrix V^{PQ}, the effective Hamiltonian coupling the P channels is approximately

$$H^{PP}_{\mathrm{eff}}\simeq-\frac{1}{2}I^{PP}\frac{d^2}{dr^2}+V^{PP}+V^{PQ}\frac{1}{g^{QQ}}V^{QP}+V^{PQ}\frac{\left[-\frac{1}{2}I^{QQ}\frac{d^2}{dr^2}-\epsilon_{P_0}(E,r)I^{QQ}\right]}{(g^{QQ})^2}V^{QP}, \tag{50}$$

where

$$g^{QQ}=\left[E_{P_0}-E_Q+\frac{\ell_{P_0}(\ell_{P_0}+1)-\ell_Q(\ell_Q+1)}{2r^2}\right]I^{QQ}. \tag{51}$$

In the following development terms higher than second order in the matrix V^{PQ} and terms involving $-\frac{1}{2}I^{QQ}d^2/dr^2-\epsilon_{P_0}(E,r)I^{QQ}$ are neglected; these are one to two orders of magnitude smaller than the first three terms in the effective Hamiltonian of Eq. (50) for the cases studied here.

In contrast to the adiabatic formulation, this diabatic approach has only a nondegenerate case since all thresholds in the P subspace are distinct from those in the Q subspace. This separation between the P and Q subspaces is due to electrostatic splitting, which is large compared to the fine-structure splitting within the P subspace. Thus we can expand the inverted matrix in Eq. (50) in powers of $\ell_{P_0}(\ell_{P_0}+1)-\ell_Q(\ell_Q+1)/2(E_{P_0}-E_Q)r^2$. Using the same approach as in Sec. II, we perform a recoupling to reveal the tensorial structure, but we do not transform to the angular-momentum representation used in Sec. II since it cannot correctly account for the coupling between the diabatic channels. Specifically, neither the $J_c^{(k)}\cdot\ell^{(k)}$ operator representation used in the adiabatic formulation nor the $L_c^{(k)}\cdot\ell^{(k)}$ representation suggested by the presence of the $\vec{L}_c\cdot\vec{\ell}$ term in the Ref. [4] derivation correctly accounts for the coupling between the diabatic channels. $J_c^{(k)}\cdot\ell^{(k)}$ requires $J_c=J_c'$ and $\ell_\mu=\ell_{\mu'}$, while $L_c^{(k)}\cdot\ell^{(k)}$ requires $L_c=L_c'$ and $\ell_\mu=\ell_{\mu'}$. Thus the $\vec{L}_c\cdot\vec{\ell}$ term predicted by Ref. [4] will only appear provided L_c is a good quantum number, which will be approximately true for low-Z atomic Rydberg systems. However, we can readily identify a similar operator structure, which we symbolically represent as $X_c^{(k)}\cdot Y_R^{(k)}$. This procedure gives an effective Hamiltonian with the following anisotropic structure

$$\begin{aligned}H^{\mu\mu'}_{\mathrm{eff}}=&\left(-\frac{1}{2}\frac{d^2}{dr^2}+E_\mu-\frac{1}{r}+\frac{\ell_\mu(\ell_\mu+1)}{2r^2}\right)\delta_{\mu\mu'}\\&+\left[\frac{C^{4\mu\mu'}_{0(1,1)}}{r^4}+\frac{C^{6\mu\mu'}_{0[(1,1),(2,2)]}}{r^6}\right]\langle X_c^{(0)}\cdot Y_R^{(0)}\rangle_{\mu\mu'}\\&+\frac{C^{6\mu\mu'}_{1(1,1)}}{r^6}\langle X_c^{(1)}\cdot Y_R^{(1)}\rangle_{\mu\mu'}+\left[\frac{C^{3\mu\mu'}_{2(2,0)}}{r^3}+\frac{C^{4\mu\mu'}_{2(1,1)}}{r^4}\right.\\&\left.+\frac{C^{6\mu\mu'}_{2[(1,1),(2,2),(1,3)]}}{r^6}\right]\langle X_c^{(2)}\cdot Y_R^{(2)}\rangle_{\mu\mu'}+\left[\frac{C^{5\mu\mu'}_{4(4,0)}}{r^5}\right.\\&\left.+\frac{C^{6\mu\mu'}_{4[(2,2),(1,3)]}}{r^6}\right]\langle X_c^{(4)}\cdot Y_R^{(4)}\rangle_{\mu\mu'},\end{aligned} \tag{52}$$

where μ and μ' indicate channels within the P subspace, while ν refers to channels in the Q subspace. The operator structure of the coupling potential in this effective Hamiltonian is similar to that of the long-range potential in Eq. (20). In fact, apart from there being no post-adiabatic contributions, the various terms in this coupling potential can be viewed as a generalization of the terms in Eq. (20).

Here the $C^{n\mu\mu'}_{k(a,b)}$ are given by

$$C^{n\mu\mu'}_{k(a,b)}=(-1)^{k+J_c+J_c'+\ell_{\mu'}}(2k+1)[(2\ell_\mu+1)(2\ell_{\mu'}+1)]^{1/2}\sum_{\gamma_\nu,J_\nu,\ell_\nu}\Lambda^n_{P_0\nu}(a,b)(-1)^{\ell_\nu}(2\ell_\nu+1)\times\{\ell_\mu,a,\ell_\nu\}\{\ell_\nu,b,\ell_{\mu'}\}\begin{Bmatrix} a & b & k\\ \ell_{\mu'} & \ell_\mu & \ell_\nu\end{Bmatrix}\times\begin{Bmatrix} a & b & k\\ J_c' & J_c & J_\nu\end{Bmatrix}\left\langle \gamma_c J_c\left\|\sum_{i=1}^{N_c} r_i^a C^{(a)}(\hat r_i)\right\|\gamma_\nu J_\nu\right\rangle\times\left\langle \gamma_\nu J_\nu\left\|\sum_{j=1}^{N_c} r_j^b C^{(b)}(\hat r_j)\right\|\gamma_c' J_c'\right\rangle, \tag{53}$$

while

$$\langle X_c^{(k)}\cdot Y_R^{(k)}\rangle_{\mu\mu'}=\langle (J_c\ell_\mu)K|X_c^{(k)}\cdot Y_R^{(k)}|(J_c'\ell_{\mu'})K\rangle \equiv(-1)^{J_c'+\ell_\mu+K}\langle J_c\|X_c^{(k)}\|J_c'\rangle\langle\ell_\mu\|Y_R^{(k)}\|\ell_{\mu'}\rangle\times\begin{Bmatrix} J_c & \ell_\mu & K\\ \ell_{\mu'} & J_c' & k\end{Bmatrix}. \tag{54}$$

$X_c^{(k)}$ and $Y_R^{(k)}$ are "unit tensorial operators" (spatial) of rank k operating on the core and Rydberg electron, respectively, with reduced matrix elements given by

$$\langle J_c\|X_c^{(k)}\|J_c'\rangle=\begin{cases}1 \text{ if } \Delta(J_c,k,J_c')\\ 0 \text{ otherwise}\end{cases} \tag{55}$$

and

$$\langle\ell_\mu\|Y_R^{(k)}\|\ell_{\mu'}\rangle=\begin{cases}1 \text{ if } \Delta(\ell_\mu,k,\ell_{\mu'})\\ 0 \text{ otherwise}\end{cases}, \tag{56}$$

where $\Delta(x,y,z)$ denotes the condition of triangularity among the quantum numbers x,y, and z. Explicit expressions for particular $\Lambda^n_{P_0\nu}(a,b)$ are

$$\Lambda^3_{P_0\nu}(2,0)=\Lambda^5_{P_0\nu}(4,0)=1, \tag{57}$$

$$\Lambda^4_{P_0\nu}(1,1)=\Lambda^6_{P_0\nu}(2,2)=\frac{1}{E_{P_0}-E_\nu}, \tag{58}$$

$$\Lambda^6_{P_0\nu}(1,3)=2\Lambda^4_{P_0\nu}(1,1), \tag{59}$$

$$\Lambda^6_{P_0\nu}(1,1)=\frac{[\ell_\nu(\ell_\nu+1)-\ell_{P_0}(\ell_{P_0}+1)]}{2(E_\nu-E_{P_0})^2}. \tag{60}$$

Once again, the operator representation of the effective Hamiltonian in Eq. (52) shows the appearance of a vector term. Here we have retained the summations over ℓ_ν that appear in the various terms to show explicitly how the vector term arises. The summation over ℓ_ν in the vector term

$$\sum_{\ell_\nu}(-1)^{\ell_\nu}[\ell_\nu(\ell_\nu+1)-\ell_{P_0}(\ell_{P_0}+1)](2\ell_\nu+1)\times\begin{pmatrix}\ell_\mu & 1 & \ell_\nu\\ 0 & 0 & 0\end{pmatrix}\begin{pmatrix}\ell_\nu & 1 & \ell_{\mu'}\\ 0 & 0 & 0\end{pmatrix}\begin{Bmatrix} 1 & 1 & 1\\ \ell_{\mu'} & \ell_\mu & \ell_\nu\end{Bmatrix} =(-1)^{1-\ell_\mu}\left[\frac{2}{3}\frac{\ell_\mu(\ell_\mu+1)}{(2\ell_\mu+1)}\right]^{1/2}\delta_{\ell_\mu\ell_{\mu'}} \tag{61}$$

is generally nonzero. In contrast, other terms that do not possess this additional $\ell_\nu(\ell_\nu+1)$ dependence share the following summation over ℓ_ν:

$$\sum_{\ell_\nu}(-1)^{\ell_\nu}(2\ell_\nu+1)\begin{pmatrix}\ell_\mu & a & \ell_\nu\\ 0 & 0 & 0\end{pmatrix}\begin{pmatrix}\ell_\nu & b & \ell_{\mu'}\\ 0 & 0 & 0\end{pmatrix}\times\begin{Bmatrix} a & b & k\\ \ell_{\mu'} & \ell_\mu & \ell_\nu\end{Bmatrix} =(-1)^{-a-b-\ell_{\mu'}-\ell_\mu+k}\begin{pmatrix}a & b & k\\ 0 & 0 & 0\end{pmatrix}\begin{pmatrix}\ell_{\mu'} & \ell_\mu & k\\ 0 & 0 & 0\end{pmatrix}. \tag{62}$$

Since only values of a and b that add up to an even number appear in the various terms, k must be even. Thus it is the centrifugal term along with the dipole moments of the core that give rise to the vector term.

A. Parametrization

Each of the $C^{n\mu\mu'}_{k(a,b)}$ terms depends on information that is specific to the channels μ and μ'. Expressing each $C^{n\mu\mu'}_{k(a,b)}$ in terms of quantities that are channel independent along with others that are channel dependent defines a parametrization of the effective Hamiltonian. Once such channel-independent quantities (such as the scalar and tensor polarizabilities) are determined for a particular Rydberg system, the effective Hamiltonian can be used efficiently to describe the interaction between a Rydberg electron and an anisotropic ionic core. The effective Hamiltonian provides a systematic method for going beyond lowest-order perturbation theory, which is often used to compute shifts of high-n and -ℓ Rydberg levels from hydrogenic levels. The effective Hamiltonian can also be used to improve upon the adiabatic approach presented in Sec. II, if desired.

In low-Z atomic systems the spin-orbit interaction is small compared to the electrostatic interaction. As a consequence, the total orbital angular momentum L_c and the total spin S_c of the core are approximately good quantum numbers. This means that low Z atomic Rydberg systems possess a set of quantum numbers that are approximately the same for all relevant channels. Decoupling $C^{n\mu\mu'}_{k(a,b)}$ into ℓ, J_c, L_c, and S_c we find

$$C^{n\mu\mu'}_{k(a,b)}=(-1)^{J'_c+S_c+L_c+\ell_{\mu'}}(2k+1)\begin{Bmatrix} k & L_c & L_c \\ S_c & J_c & J'_c \end{Bmatrix}[(2\ell_\mu+1)(2\ell_{\mu'}+1)(2J_c+1)(2J'_c+1)]^{1/2}$$
$$\times\sum_{n_\nu,L_\nu,\ell_\nu}\Lambda^n_{P_0\nu}(a,b)(-1)^{\ell_\nu}(2\ell_\nu+1)\{\ell_\mu,a,\ell_\nu\}\{\ell_\nu,b,\ell_{\mu'}\}\begin{Bmatrix} a & b & k \\ \ell_{\mu'} & \ell_\mu & \ell_\nu \end{Bmatrix}\begin{Bmatrix} k & L_c & L_c \\ L_\nu & a & b \end{Bmatrix}$$
$$\times\left\langle n_cL_c\left\|\sum_{i=1}^{N_c} r_i^a C^{(a)}(\hat r_i)\right\|n_\nu L_\nu\right\rangle\left\langle n_\nu L_\nu\left\|\sum_{j=1}^{N_c} r_j^b C^{(b)}(\hat r_j)\right\|n_cL_c\right\rangle. \tag{63}$$

With this decoupling the various terms in our effective Hamiltonian take on a parametrized form. For example, $C^{4\mu\mu'}_{0(1,1)}$ is simply related to the standard dipole scalar polarizability α_s [21] through

$$C^{4\mu\mu'}_{0(1,1)}\langle X^{(0)}_c\cdot Y^{(0)}_R\rangle_{\mu\mu'}=-\frac{\alpha_s}{2}, \tag{64}$$

while $C^{3\mu\mu'}_{2(2,0)}$ and $C^{4\mu\mu'}_{2(1,1)}$ are related, respectively, to the quadrupole moment Q and the second-rank tensor polarizability α_t by

$$C^{3\mu\mu'}_{2(2,0)}\langle X^{(2)}_c\cdot Y^{(2)}_R\rangle_{\mu\mu'}=-Q\mathscr{A}^{(2)}_{\mu\mu'} \tag{65}$$

and

$$C^{4\mu\mu'}_{2(1,1)}\langle X^{(2)}_c\cdot Y^{(2)}_R\rangle_{\mu\mu'}=-\frac{\alpha_t}{2}\mathscr{A}^{(2)}_{\mu\mu'}, \tag{66}$$

where the angular factor $\mathscr{A}^{(2)}_{\mu\mu'}$ is

$$\mathscr{A}^{(2)}_{\mu\mu'}=(-1)^{2J'_c+L_c+S_c+K}[(2\ell_\mu+1)(2\ell_{\mu'}+1)(2J_c+1)$$
$$\times(2J'_c+1)]^{1/2}\begin{Bmatrix} J_c & \ell_\mu & K \\ \ell_{\mu'} & J'_c & 2 \end{Bmatrix}\begin{Bmatrix} 2 & L_c & L_c \\ S_c & J_c & J'_c \end{Bmatrix}$$
$$\times\begin{pmatrix} \ell_{\mu'} & \ell_\mu & 2 \\ 0 & 0 & 0 \end{pmatrix}\Big/\begin{pmatrix} L_c & 2 & L_c \\ -L_c & 0 & L_c \end{pmatrix}. \tag{67}$$

In addition, the vector term $C^{6\mu\mu'}_{1(1,1)}\langle X^{(1)}_c\cdot Y^{(1)}_R\rangle_{\mu\mu'}$ can be expressed in terms of a vector hyperpolarizability β_v by

$$C^{6\mu\mu'}_{1(1,1)}\langle X^{(1)}_c\cdot Y^{(1)}_R\rangle_{\mu\mu'}=\beta_v\langle\vec L_c\cdot\vec\ell\rangle_{\mu\mu'}, \tag{68}$$

where β_v is defined by

$$\beta_v\equiv\frac{\sqrt{6}}{[L_c(L_c+1)(2L_c+1)]^{1/2}}\sum_{n_\nu,L_\nu}\frac{1}{2(E_\nu-E_{P_0})^2}\begin{Bmatrix} 1 & L_c & L_c \\ L_\nu & 1 & 1 \end{Bmatrix}\left\langle n_cL_c\left\|\sum_{i=1}^{N_c} r_iC^{(1)}(\hat r_i)\right\|n_\nu L_\nu\right\rangle$$
$$\times\left\langle n_\nu L_\nu\left\|\sum_{j=1}^{N_c} r_jC^{(1)}(\hat r_j)\right\|n_cL_c\right\rangle \tag{69}$$

and

$$\langle\vec L_c\cdot\vec\ell\rangle_{\mu\mu'}=\langle[(L_cS_c)J_c\ell_\mu]K|\vec L_c\cdot\vec\ell|[(L_cS_c)J'_c\ell_{\mu'}]K\rangle=(-1)^{L_c+S_c+2J'_c+\ell_\mu+1+K}[(2J_c+1)(2J'_c+1)]^{1/2}\langle L_c\|L^{(1)}_c\|L_c\rangle$$
$$\times\langle\ell_\mu\|\ell^{(1)}\|\ell_{\mu'}\rangle\begin{Bmatrix} L_c & J_c & S_c \\ J'_c & L_c & 1 \end{Bmatrix}\begin{Bmatrix} J_c & \ell_\mu & K \\ \ell_{\mu'} & J'_c & k \end{Bmatrix}. \tag{70}$$

Our use of the terminology ''hyperpolarizability'' is intended to emphasize the difference between the term involving β_v, which varies as r^{-6}, from the more familiar terms involving α_s and α_t, which vary as r^{-4}.

The remaining $C^{6\mu\mu'}_{0[(1,1),(2,2)]}$ and $C^{6\mu\mu'}_{2[(1,1),(2,2),(1,3)]}$ terms are related, respectively, to the parameters η and c_6 [7] by

$$C^{6\mu\mu'}_{0[(1,1),(2,2)]}\langle X^{(0)}_c\cdot Y^{(0)}_R\rangle_{\mu\mu'}=-\eta \tag{71}$$

and

$$C^{6\mu\mu'}_{2[(1,1),(2,2),(1,3)]}\langle X^{(2)}_c\cdot Y^{(2)}_R\rangle_{\mu\mu'}=-c_6\mathscr{A}^{(2)}_{\mu\mu'}. \tag{72}$$

Thus the effective diabatic Hamiltonian in parametrized form is

$$H^{\mu\mu'}_{\rm eff}=\left(-\frac{1}{2}\frac{d^2}{dr^2}+E_\mu-\frac{1}{r}+\frac{\ell_\mu(\ell_\mu+1)}{2r^2}\right)\delta_{\mu\mu'}-\frac{\alpha_s}{2r^4}-\frac{\eta}{r^6}$$
$$+\frac{\beta_v}{r^6}\langle\vec L_c\cdot\vec\ell\rangle_{\mu\mu'}-\left[\frac{Q}{r^3}+\frac{\alpha_t}{2r^4}+\frac{c_6}{r^6}\right]\mathscr{A}^{(2)}_{\mu\mu'}. \tag{73}$$

Here the choice of the $\vec{L}_c \cdot \vec{\ell}$ operator representation is appropriate since the general vector term in Eq. (52) requires $\ell_\mu = \ell_{\mu'}$ and since we are considering low-Z atomic Rydberg systems where L_c is an approximately good quantum number.

B. Numerical results using a Sturmian basis set

The study of high-n and -ℓ Rydberg systems with low-Z atomic numbers has now been reduced to the determination of a few parameters ($\alpha_s, \alpha_t, Q, \beta_v, \ldots$) that characterize the ionic cores of these systems. With these parameters energy levels and adiabatic potentials (treating the radial coordinate as a parameter) can be computed by diagonalizing the effective Hamiltonian. In addition, dynamical information can be obtained by solving a set of coupled radial equations.

The parameters that characterize the ionic cores of Rydberg systems can be computed from first principles or extracted from Rydberg energy levels. In this section we demonstrate how these parameters for Ne^+ can be obtained from the $n=10$ Rydberg levels of neon with $\ell=5,6,7$, and 8, which have been studied in recent experiments by Ward *et al.* [7]. This is accomplished by minimizing the weighted χ^2 function, involving differences between the observed and computed energy levels, with respect to the parameters $\alpha_s, \alpha_t, Q, \beta_v, \ldots$.

To diagonalize the effective Hamiltonian we use a complete basis of radial Sturmians

$$S_{n\ell}^{(\zeta)}(r) = \left[\frac{(n-\ell-1)!}{(n+\ell)!}\right]^{1/2} e^{-\zeta r/2}(\zeta r)^{\ell+1} L_{n-\ell-1}^{(2\ell+1)}(\zeta r), \tag{74}$$

where the $L_{n-\ell-1}^{(2\ell+1)}(\zeta r)$ are associated Laguerre polynomials defined by

$$L_n^{(k)}(x) = \sum_{\nu=0}^{n} \binom{n+k}{n-\nu} \frac{(-x)^\nu}{\nu!} \tag{75}$$

and ζ is a parameter chosen to enhance convergence. After we write F_P as a linear combination of these Sturmian functions, the close-coupling equation for F_P becomes a generalized eigenvalue problem

$$H_{\text{eff}}\Psi = EO\Psi, \tag{76}$$

where H_{eff} and O are the effective Hamiltonian and overlap matrices in the Sturmian basis [17]. We use a Sturmian basis set, in contrast to the perturbative calculation scheme developed by Ref. [7], in part because of its simplicity and in part because it naturally incorporates coupling to the continuum states.

In order to compare the computed energies with experimentally observed energies, relativistic contributions must be added to the energies obtained from the nonrelativistic effective Hamiltonian. Since the experimentally observed spin splittings are only partially resolved, all spin-orbit and exchange terms are neglected. The dominant relativistic contributions come from the p^4 term in the kinetic energy of the Rydberg electron and the magnetic interaction between the Rydberg electron and the ionic core given by

$$H_{\text{mag}} = -\frac{g_J}{2}\alpha^2 \frac{\vec{J}_c \cdot \vec{\ell}}{r^3}, \tag{77}$$

where α is the fine-structure constant and g_J is the g factor of the ionic core. The following calculations include these relativistic contributions perturbatively. All energies are shifted so that the state $(3/2)10K_{15/2}$ corresponds to zero energy.

Table I compares our results for the various parameters (e.g., polarizabilities, quadrupole moment, and hyperpolarizabilities) of Ne^+ with those of Ward *et al.* [7]. The striking difference between our results and those of Ref. [7] is the 80% improvement in the χ^2 associated with our parameters. The fact that the χ^2-squared per degree of freedom (per parameter) is now approximately *one* is a clear indication that the anisotropic interaction potential correctly accounts for the distribution of Rydberg energy levels. Columns 2, 3, and 4 of Table II compare the improved energy eigenvalues from our diagonalization with the measured energy levels of Ref. [7] for $n=10$ Rydberg states of neon with $\ell=5,6,7$, and 8. This diagonalization utilized 40 radial Sturmian functions per channel, $\zeta = 1/(\ell+1)$, and all our parameters listed in Table I. These parameters reproduce all observed energy levels to better than 1 MHz.

In order to ascertain whether the Ref. [7] experiment has actually observed effects of the vector hyperpolarizability term β_v, we have repeated the same analysis described in the preceding paragraph *except* that β_v was constrained to vanish. The resulting refitted parameters are given in Table I (except of course for the omitted β_v). The coefficient g_J, which represents the gyromagnetic ratio of the $Ne^+(^2P_{3/2})$ level, changes by the greatest amount in this fit, going from 1.342 to 1.307. Inspection of Eq. (77) shows that the tensorial structure of the g_J term is similar to that of the β_v term, so it is reasonable that the new fit modifies g_J in order to "mock up" the effects of the omitted vector hyperpolarizability. Note also that the value of g_J expected in LS coupling is precisely 4/3. (Its value could be measured independently to test the fitted value in Table I, e.g., by a linear Zeeman effect measurement.) Columns 2, 5, and 6 of Table II compare the energy eigenvalues obtained from these fitted parameters, with β_v constrained to vanish, with the measured levels of Ref. [7]. The larger discrepancies between observed and computed energies appear in states with lower-ℓ values, the largest of which is -1.43 MHz in $(3/2)10H_{9/2}$. The new least-squares fit omitting β_v results in $\chi^2 = 27.5$. Thus the χ^2 per degree of freedom is roughly four times worse than in the fit including β_v. This strongly suggests that the Ward *et al.* [7] experiment has indeed observed the vector hyperpolarizability.

Figures 1 and 2 display two sets of adiabatic potentials for neon that exhibit qualitative differences. In Fig. 1 the adiabatic potentials correspond to $K^\pi = 9/2^-$ and are labeled from top to bottom with $(J_c, \ell) = (1/2,5)$, $(3/2,5)$, and $(3/2,3)$. The absence of avoided crossings and the smoothly decaying behavior of the derivative couplings justify the use of an adiabatic treatment. Other sets of adiabatic potentials for different symmetries can differ in a crucial manner. For instance, Fig. 2 shows a set of adiabatic potentials corresponding to $K^\pi = 11/2^-$ that are labeled from top to bottom

TABLE I. Comparison of fitted (experimental) and theoretical parameters for Ne^+. L refers to length form and V refers to velocity form. The value of g_J in column 5 (marked with an asterisk) is based on pure LS coupling.

Parameter	Present fit	Present fit without β_v	Ward *et al.*	Theoretical
α_s	1.3018(2)	1.3011(6)	1.3028(13)	1.23 (L) 1.19 (V) 1.27 [a]
α_t	−0.0259(3)	−0.0261(3)	−0.026(5)	−0.0374 (L) −0.0396 (V) −0.035 [b]
Q	−0.204020(5)	−0.204001(11)	−0.20403(5)	−0.1964 [c] −0.2032(5) [c] −0.2117 [b]
β_v	0.059(2)	0	0.045(29)	0.0678 (L) 0.0719 (V)
η	−0.10(1)	−0.10(1)	−0.29(24)	−1.44 [d]
g_J	1.342(12)	1.307(24)	1.354(21)	4/3 *
c_6	0.274(5)	0.264(3)	0.5(5)	
χ^2	7.1	27.5	35.7	

[a]Reference [19].
[b]Reference [13].
[c]Reference [18].
[d]Reference [20].

with $(J_c,\ell) = (1/2,5)$, $(3/2,7)$, and $(3/2,5)$. Here the presence of a close avoided crossing and a corresponding sharp derivative coupling introduce numerical difficulties in a pure adiabatic formulation. The effective Hamiltonian approach bypasses numerical difficulties associated with derivative couplings in an adiabatic formulation by essentially treating the dynamics adiabatically only within the Q subspace. This approach preserves the simple form of a set of coupled di-

TABLE II. Comparison of calculated (with and without β_v) and experimentally observed energies in (MHz) of $n=10$ Rydberg neon with $J_c=3/2$ and $\ell=5,6,7$, and 8. $\Delta E = E_{\rm obs} - E_{\rm calc}$.

States	$E_{\rm obs}$ [7]	$E_{\rm calc}$	ΔE	$E_{\rm calc}^{\beta_v=0}$	$\Delta E^{\beta_v=0}$
$H_{9/2}$	−145.58(77)	−145.63	0.05	−144.15	−1.43
$H_{11/2}$	2142.67(10)	2142.60	0.07	2142.81	−0.14
$H_{13/2}$	−6022.24(19)	−6022.02	0.22	−6022.66	0.42
$I_{9/2}$	−5267.15(35)	−5267.38	0.23	−5266.64	−0.51
$I_{11/2}$	−356.30(24)	−356.18	−0.12	−355.91	−0.39
$I_{13/2}$	800.52(5)	800.50	0.02	800.55	−0.03
$I_{15/2}$	−4131.36(15)	−4131.35	−0.01	−4131.10	−0.26
$K_{11/2}$	−3838.06(35)	−3838.50	0.44	−3838.26	0.20
$K_{13/2}$	−646.41(8)	−646.37	−0.04	−646.36	−0.05
$K_{15/2}$	0	0	0	0	0
$K_{17/2}$	−3205.01(16)	−3204.97	−0.04	−3204.68	−0.33
$L_{13/2}$	−3073.14(35)	−3073.64	0.50	−3073.56	0.42
$L_{15/2}$	−883.09(8)	−883.04	−0.05	−883.08	−0.01
$L_{17/2}$	−494.04(5)	−494.04	0.00	−494.05	0.01
$L_{19/2}$	−2693.41(18)	−2693.38	−0.03	−2693.14	−0.27

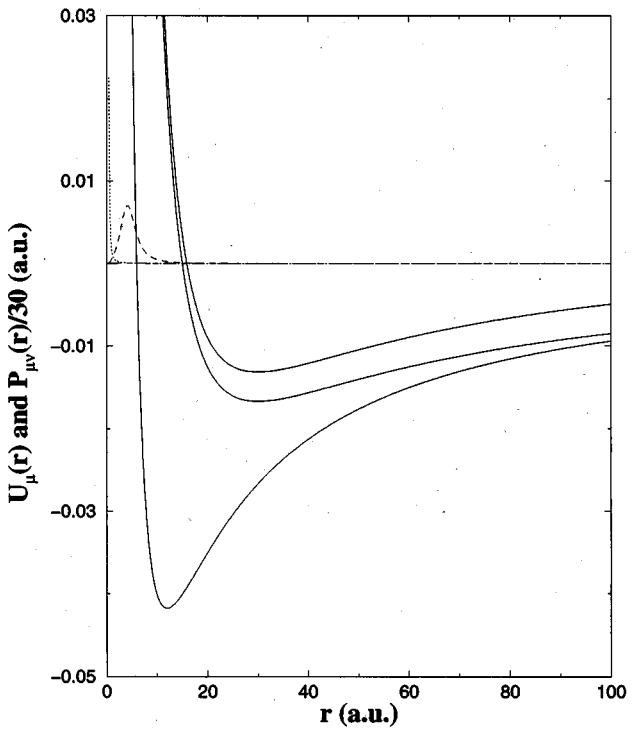

FIG. 1. Adiabatic potentials and derivative couplings for Rydberg neon. The adiabatic potentials $U_\mu(r)$ (solid lines) correspond to $K^\pi = 9/2^-$ and are labeled from top to bottom with $(J_c, \ell) = (1/2,5), (3/2,5)$, and $(3/2,3)$. The derivative couplings $P_{\mu\nu}(r)/30$ are given by broken lines: $P_{\text{top, middle}}(r)$, dashed; $P_{\text{middle, bottom}}(r)$, dotted and $P_{\text{top,bottom}}(r)$, dot-dashed.

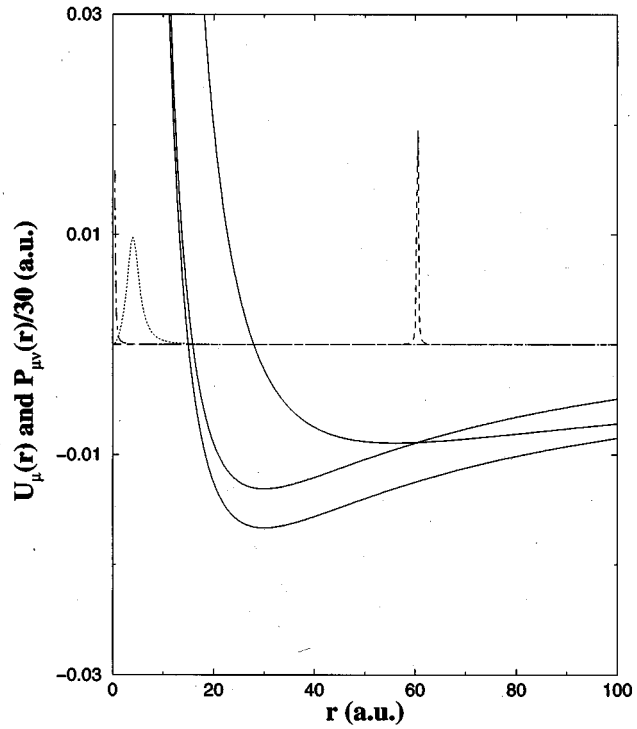

FIG. 2. Adiabatic potentials and derivative couplings for Rydberg neon. The adiabatic potentials $U_\mu(r)$ (solid lines) correspond to $K^\pi = 11/2^-$ and are labeled from top to bottom with $(J_c, \ell) = (1/2,5), (3/2,7)$, and $(3/2,5)$. The derivative couplings $P_{\mu\nu}(r)/30$ are given by broken lines: $P_{\text{top, middle}}(r)$, dashed; $P_{\text{middle, bottom}}(r)$, dotted; and $P_{\text{top,bottom}}(r)$, dot-dashed.

abatic equations in the P subspace while still incorporating a physically useful parametrization of the long-range interactions.

While an adiabatic formulation can suffer from numerical difficulties, adiabatic potentials can be used to qualitatively understand both simple and complex spectra. The wave function of a Rydberg electron moving in the presence of these potentials will be distributed among the various channels (paths). The combination of amplitudes from the various paths can result in interference and consequently complex spectra. The degree to which this takes place depends on the coupling between channels and whether the channels support strongly overlapping series converging to the various thresholds. The adiabatic potentials in Figs. 1 and 2 converging to the $P_{1/2}$ and $P_{3/2}$ states of neon may give rise to such complex spectra. This present effective Hamiltonian approach is well suited to the description of such phenomena, especially in conjunction with multichannel quantum-defect theory.

C. Calculation of vector hyperpolarizability

In this subsection we discuss the calculation of the reduced dipole matrix elements necessary to evaluate the vector hyperpolarizability β_v along with the standard dipole scalar polarizability α_s and the second-rank tensor polarizability α_t of Ne^+. The theoretical values for α_s, α_t, and β_v are presented in both length and velocity form in Table I for comparison with other theoretical and experimental results.

Here reduced dipole matrix elements are calculated for the ground state of $Ne^+(2s^2 2p^5\ ^2P^o)$. The dipole operator $r^{(1)}C_q^{(1)}$ connects states of the opposite parity that differ by at most one orbital and such that $\Delta L_c = 0, \pm 1$ (except for $L_c = 0$ to $L_c = 0$ transitions) and $\Delta S_c = 0$. Thus only the ^2S, ^2P, and ^2D final states are needed, which are generated from the ground state by $2s \rightarrow np$, $2p \rightarrow ns$, and $2p \rightarrow nd$ substitutions. Excitations of the $1s$ core are ignored since these give negligible contributions to reduced dipole matrix elements. These final states of Ne^+ are represented by $2s2p^6$, $2s2p^5np$, $2s^2 2p^4 ns$, and $2s^2 2p^4 nd$ configurations, which can be constructed (including the ground state $2s^2 2p^5$) from a product of Ne^{2+} states $2s2p^5$ or $2s^2 2p^4$, and an outer s, p, or d electron. These Ne^{2+} configurations are referred to as *physical* target states. The summations over bound and continuum states of Ne^+ are accomplished using the eigenchannel R-matrix method [22]. This allows us to construct a complete set of orthogonal basis functions, vanishing inside the R-matrix sphere of radius r_0. Such functions represent a bound spectrum and a discretized continuum of Ne^+.

The target states of Ne^{2+} are calculated using the multiconfiguration Hartree-Fock approximation [23], where both spectroscopic and correlation orbitals are included. First, spectroscopic orbitals $1s$, $2s$, and $2p$ are optimized on a single $2s^2 2p^4$ configuration. Then, a correlation $\underline{3d}$ orbital is optimized on $2s2p^5\ ^3P^o$, whose configuration-interaction (CI) expansion includes the main perturber $2s^2 2p^3 3d\ ^3P^o$. Finally, $\underline{3s}$ and $\underline{3p}$ correlation orbitals are optimized on $2s^2 2p^4\ ^3\underline{P}$, where singly and doubly excited configurations allowed by parity and spin-angular-momentum coupling

TABLE III. Theoretical and experimental energies [24] in cm^{-1} (upper and lower entries in first column, respectively) of some Ne^{2+} states, relative to the ground state $2s^22p^4\ ^3P$, and shortened CI expansions for each of these states.

Energy	Composition		
0.0	$2s^22p^4\ ^3P$	$2s2p^4(^2D)3d\ ^3P$	$2s2p^4(^2P)3d\ ^3P$
0.0	0.98605	0.00410	0.00160
25559	$2s^22p^4\ ^1D$	$2s2p^4(^2P)3d\ ^1D$	$2s^22p^2(^1D)3p^2(^3P)^1D$
25521	0.98406	0.00672	0.00176
53096	$2s^22p^4\ ^1S$	$2p^6\ ^1S$	$2s^22p^2(^1S)3d^2(^1S)\ ^1S$
55427	0.95453	0.03386	0.00303
203471	$2s2p^5\ ^3P$	$2s^22p^3(^2D)3d\ ^3P$	$2s^22p^3(^2P)3d\ ^3P$
204589	0.97417	0.01000	0.00397
291435	$2s2p^5\ ^1P$	$2s^22p^3(^2D)3d\ ^1P$	$2s^22p^3(^2P)3d\ ^1P$
289159	0.96629	0.01300	0.00314

rules are included. We then set up an initial, long CI expansion for each LS term in the $2s^22p^4$ and $2s2p^5$ configuration, including all allowed (by parity and LS-symmetry conservation rules) singly and doubly excited configurations of $2s$, $2p$, $\underline{3s}$, $\underline{3p}$, and $\underline{3d}$ orbitals. After diagonalizing a Hamiltonian, this initial CI set is condensed; from each eigenvector representing a physical target state, we delete those configurations whose weight is less than 0.0005. In the final step, extra configurations representing the target polarization are added. These are constructed from single-electron excitations from $2s^22p^4$ and $2s2p^5$, involving a change in the parity as $2s\rightarrow 2p$, $2p\rightarrow 3s$, and $2p\rightarrow 3d$. Table III shows energies and dominant configurations for each physical target state in the condensed basis. Comparing with experiment [24], our relative energies are accurate to at least 5%.

As in previous eigenchannel R-matrix calculations [22,25], a discretized basis of outer-electron orbitals ns, np, nd, nf, and ng are used. These are solved for inside the R-matrix sphere of radius $r_0=7$ Bohr radii. The size of r_0 is chosen to match all physical target states and the ground state of Ne^+ and to ensure an exponential decay of $rP_{nl}(r)$, where $P_{nl}(r)$ are the ground-state radial functions. Radial functions for an outer electron are obtained from a Hartree equation

$$\left(-\frac{1}{2}\frac{d^2}{dr^2}+\frac{l(l+1)}{2r^2}-\frac{Z}{r}+V_H(r)\right)P_{nl}(r)$$

$$=E_{nl}P_{nl}(r)+\sum_{n'}\lambda_{nn'}P_{n'l}(r),$$

where

$$V_H(r)=\sum_{n'}q_{n'l}\left[\int_0^{r_0}\frac{1}{r_>}P_{n'l}^2(s)ds\right],$$

where $r_>$ is the greater of the radial r and s coordinates, $q_{n'l}$ are occupation numbers of spectroscopic orbitals representing the $2s^22p^4$ target, and $\lambda_{nn'}$ are Lagrange multipliers needed to orthogonalize the outer-electron and target orbitals (including the correlation orbitals). All new ''box'' orbitals are forced to vanish at the R-matrix surface. These constitute a complete orthogonal basis, representing an electron outside the residual Ne^{2+} ion. Those orbitals, which have positive energies $E_{nl}>-Z_{\rm eff}/r_0+l(l+1)/2r_0^2$, describe not only bound states but also represent a discretized continuum of the Ne^+ spectrum.

The ground state of Ne^+ is constructed from an antisymmetrized product of the target states and outer-electron orbitals. The energies and atomic wave functions of Ne^+ are just eigenvalues and eigenvectors, respectively, of the Hamiltonian. The ionization energy of $Ne^+(2s^22p^5\ ^2P^o)$ obtained in this calculation is 334 460 cm^{-1}, whereas the experimental value is 331 350 cm^{-1}. A better check of accuracy based on an analysis of errors in quantum defects provides information about the whole Rydberg series, not just one member. The theoretical and experimental effective quantum numbers of a $2p$ electron in $2s^22p^5\ ^2P^o$ are 0.573 and 0.572, respectively, giving a difference of 0.001 in the quantum defect.

The final ^2S, ^2P, and ^2D states are constructed in the same way as the ground state. However, a similar estimate of errors can only be made for the lowest eigenstates whose atomic wave functions fit inside 7 Bohr radii and thus represent physical states of Ne^+. For the lowest, even-parity state $2s2p^6\ ^2S$ we obtain an excitation energy of 215 953 cm^{-1}, where as the experimental energy is 217 050. The corresponding error in the quantum defect is only 0.01, well within the range of errors expected for such a strongly correlated state. Note that $2s2p^6\ ^2S$ is correlated predominantly with a $2s^22p^4\underline{3d}^2S$ perturber, which contributes nearly 25% of the CI expansion. No similar error analysis can be carried out for higher excited states, of course, since those no longer fit into the R-matrix box.

Our final results are obtained with 11 orbitals for each angular momentum l. However, a different number of the box orbitals was initially used to test convergence of the dipole scalar polarizability. For the ^2S and ^2P symmetries, whose calculations consume the least computer CPU time and memory, we increased the number of box states to 13. This changed the scalar polarizability by about 2%. We also tested the importance of g waves, since these, along with f waves, were neglected in earlier theoretical calculations [18]. The g waves were found to contribute about 3% to the scalar dipole polarizability and even greater effects are expected from f waves. Therefore, these are kept in the present calculations. Our final value of the scalar polarizability is 1.23 a.u. in length form and 1.19 a.u. in velocity form. The scalar polarizability in length form differs by about 6% with experimental results and by about 3% with other theoretical results (see Table I). In velocity form, the scalar polarizability differs by about 9% with experimental results and by about 6% with theoretical results. The slightly better results obtained in Ref. [18] can be attributed to the use of a fully variational method to generate Ne^+ states, where the infinite summation over Rydberg series and continua is implicitly included, whereas our method uses a CI approach that is in general slower converging.

IV. SUMMARY

The impetus for this work was our desire to understand the physical origin of a nonrelativistic ''spin-orbit-type'' potential predicted by Zygelman [4] to exist in Rydberg systems. This unusual potential, purely electrostatic in nature despite the spin-orbit-type structure, was not given fully in the Ref. [4] derivation and until now its physical origin has remained unclear. The present study has not only clarified the physical origin of this potential but it has also spawned a reformulation and extension of existing theory to permit a description of Rydberg electron motion in the field of an anisotropic core.

Section II of this paper reformulates the conventional adiabatic derivation of the large-r interaction potential between a Rydberg electron and an open-shell ionic core. The use of recoupling algebra and a transformation to an angular-momentum operator representation reveals the anisotropic nature of the interaction. The resulting potential immediately shows the appearance of a vector contribution similar in structure to that predicted in Ref. [4]. The vector contribution depends on dipole matrix elements of the ionic core; its existence hinges on the centrifugal repulsion experienced by the Rydberg electron. Explicit expressions for all terms are given, in forms suitable to either *ab initio* calculation or semiempirical analysis of experimental spectra. An additional type of vector hyperpolarizability, not considered in Ref. [4], is predicted to occur in Rydberg systems with degenerate channels converging to the same ionization threshold. This ''degenerate vector hyperpolarizability'' interaction leads to an even stronger anisotropic potential at large distances, proportional to r^{-4}.

Section III derives an effective Hamiltonian that can be treated diabatically within a small, physically relevant channel subspace. The anisotropic nature of the interaction potential is expressed through a defined set of ''unit tensorial operators'' that correctly account for the coupling between the diabatic channels. The vector term was shown to be proportional to $\vec{L}_c \cdot \vec{\ell}$, as predicted in Ref. [4], in low-Z atomic Rydberg systems. We leave the problem of elucidating the qualitative nature of this vector term in the long-range potential for future studies. We note, however, that a term of this tensorial structure, $A\vec{L}_c \cdot \vec{\ell}$, was introduced into atomic spectroscopy by Trees and Racah, on semiempirical grounds and without explicit derivation [26,27].

This Hamiltonian was applied to the study of low-Z Rydberg systems where the parametrization resulted in a simplified description of the interaction. The effective Hamiltonian was diagonalized in a Sturmian basis set and its parameters were fitted to match recent experimental observations. This procedure determines the parameters (e.g., polarizabilities, quadrupole moment, and hyperpolarizabilities) of Ne^+ in terms of the $n=10$ Rydberg level energies of neon. This analysis provides improved values for the parameters, as evidenced by an 80% reduction in the χ^2 associated with the parameters presented in Ref. [7]. The r^{-6} potential term involving the vector hyperpolarizability significantly improves agreement between the computed and observed energy levels.

Adiabatic potentials for Rydberg channels of neon, computed with the effective Hamiltonian, show close avoided crossings that imply the existence of complex multichannel spectra. Such systems can be described effectively by using the effective Hamiltonian in conjunction with multichannel quantum defect theory.

Finally, Sec. IV presents a quantitative, *ab initio* calculation of the vector hyperpolarizability β_v for an anisotropic ion. The calculated value for Ne^+ is in reasonably good agreement with the value deduced from recent measurements of Ne Rydberg levels. Future experimental and theoretical studies will help greatly to better understand the importance of the vector hyperpolarizability and other anisotropic interactions in Rydberg systems. Candidate systems must have anisotropic cores and, if possible, should be more polarizable than Ne^+, such as Si, P, Cl, and Ar.

A recent experiment of Ekstrom *et al.* [28] utilized an atom interferometer to measure the ground-state scalar polarizability of sodium to an accuracy of 0.3%. This unusually accurate technique permitted Ref. [28] to test theoretical polarizability calculations quite stringently. Tests of this type are important, as atomic theory plays a vital role in the interpretation of many phenomena, including atomic parity-violation experiments. The present analysis demonstrates how high-precision measurements of Rydberg spectra, when combined with an appropriate description of the long-range multipole interactions, can determine ionic multipole moments to even higher accuracy than was achieved by Ref. [28]. Atomic theory can thus play two key roles in the analysis: (i) formulation of the *structure* of the long-range interaction between an electron and the ionic core, which has been the main theme of the present paper, and (ii) *ab initio* calculation of the relevant multipole moments. We have calculated three of these moments here at a relatively crude level of approximation. This shows that these moments can be quantitatively evaluated, even terms such as the vector hyperpolarizability; we anticipate that they can be determined to much higher accuracy in future experimental and theoretical studies.

ACKNOWLEDGMENTS

We would like to thank S.R. Lundeen for his encouraging and helpful discussions and J.L. Bohn for a number of insightful comments. This work has been supported in part by the National Science Foundation.

[1] M.J. Seaton and L. Steenman-Clark, J. Phys. B **10**, 2639 (1977).
[2] A. Dalgarno, G.W.F. Drake, and G.A. Victor, Phys. Rev. **176**, 194 (1968).
[3] R.J. Drachman, Phys. Rev. A **26**, 1228 (1982).
[4] B. Zygelman, Phys. Rev. Lett. **64**, 256 (1990).
[5] S. Watanabe and C.H. Greene, Phys. Rev. A **22**, 158 (1980).
[6] U. Fano and J.H. Macek, Rev. Mod. Phys. **45**, 553 (1973).
[7] R.F. Ward, Jr., W.G. Sturrus, and S.R. Lundeen (unpublished).
[8] L. Pruvost, P. Camus, J.M. Lecomte, C.R. Mahon, and P. Pillet, J. Phys. B **24**, 4723 (1991).
[9] M.J. Seaton, Proc. Phys. Soc. London **77**, 174 (1961).

[10] M. Gailitis and R. Damburg, Proc. Phys. Soc. London **82**, 192 (1963).
[11] H. Klar and U. Fano, Phys. Rev. Lett. **37**, 1132 (1976).
[12] H. Klar, Phys. Rev. A **15**, 1452 (1977).
[13] V. Aquilanti, S. Cavalli, and M.B. Sevryuk, J. Math. Phys. **35** (2), 536 (1994).
[14] R.N. Zare, *Angular Momentum* (Wiley, New York, 1988).
[15] D.A. Varshalovich, A.N. Moskalev, and V.K. Khersonskii, *Quantum Theory of Angular Momentum* (World Scientific, Singapore, 1988).
[16] U. Fano and A.R.P. Rau, *Atomic Collisions and Spectra* (Academic, Orlando, 1986).
[17] C.W. Clark and K.T. Taylor, J. Phys. B **15**, 1175 (1982).
[18] A. Hibbert, M. Le Dourneuf, and Vo Ky Lan, J. Phys. B **10**, 1015 (1977).
[19] D. Sundholm and J. Olsen, Phys. Rev. A **49**, 3453 (1994).
[20] E.S. Chang, W.G. Schoenfeld, E. Biemont, P. Quinet, and P. Palmeri, Phys. Scr. **49**, 26 (1994).
[21] W.G Schoenfeld, Ph.D. thesis, University of Massachusetts, 1994 (unpublished).
[22] C.H. Greene, *Fundamental Processes of Atomic Dynamics* (Plenum, New York, 1988), p. 105; C.H. Greene and L. Kim, Phys. Rev. A **38**, 5953 (1988); F. Robicheaux and C. H. Greene, *ibid.* **46**, 3821 (1992).
[23] C. Froese Fischer, Comput. Phys. Commun. **64**, 369 (1991).
[24] C.E. Moore, *Atomic Energy Levels*, Natl. Bur. Stand. Ref. Data. Ser., Nat. Bur. Stand. (U.S.) Circ. No. 35 (U.S. GPO, Washington, DC, 1971) Vol. I.
[25] G. Miecznik and C.H Greene (unpublished).
[26] R.E. Trees, Phys. Rev. **83**, 756 (1951); **84**, 1089 (1951); **85**, 382 (1952).
[27] G. Racah, Phys. Rev. **85**, 381 (1952).
[28] C.R. Ekstrom, J. Schmiedmayer, M.S. Chapman, T.R. Hammond, and D.E. Pritchard, Phys. Rev. A **51**, 3883 (1995).